NASA/TM-20205007197 AIAA–2020–3676

An Electrical Modeling and Thermal Analysis Toolbox for Electrified Aircraft Propulsion Simulation

Mark E. Bell
HX5, LLC, Brook Park, Ohio

Jonathan S. Litt
Glenn Research Center, Cleveland, Ohio

November 2020

NASA STI Program . . . in Profile

Since its founding, NASA has been dedicated to the advancement of aeronautics and space science. The NASA Scientific and Technical Information (STI) Program plays a key part in helping NASA maintain this important role.

The NASA STI Program operates under the auspices of the Agency Chief Information Officer. It collects, organizes, provides for archiving, and disseminates NASA's STI. The NASA STI Program provides access to the NASA Technical Report Server—Registered (NTRS Reg) and NASA Technical Report Server—Public (NTRS) thus providing one of the largest collections of aeronautical and space science STI in the world. Results are published in both non-NASA channels and by NASA in the NASA STI Report Series, which includes the following report types:

- TECHNICAL PUBLICATION. Reports of completed research or a major significant phase of research that present the results of NASA programs and include extensive data or theoretical analysis. Includes compilations of significant scientific and technical data and information deemed to be of continuing reference value. NASA counter-part of peer-reviewed formal professional papers, but has less stringent limitations on manuscript length and extent of graphic presentations.

- TECHNICAL MEMORANDUM. Scientific and technical findings that are preliminary or of specialized interest, e.g., "quick-release" reports, working papers, and bibliographies that contain minimal annotation. Does not contain extensive analysis.

- CONTRACTOR REPORT. Scientific and technical findings by NASA-sponsored contractors and grantees.

- CONFERENCE PUBLICATION. Collected papers from scientific and technical conferences, symposia, seminars, or other meetings sponsored or co-sponsored by NASA.

- SPECIAL PUBLICATION. Scientific, technical, or historical information from NASA programs, projects, and missions, often concerned with subjects having substantial public interest.

- TECHNICAL TRANSLATION. English-language translations of foreign scientific and technical material pertinent to NASA's mission.

For more information about the NASA STI program, see the following:

- Access the NASA STI program home page at http://www.sti.nasa.gov

- E-mail your question to help@sti.nasa.gov

- Fax your question to the NASA STI Information Desk at 757-864-6500

- Telephone the NASA STI Information Desk at 757-864-9658

- Write to:
  NASA STI Program
  Mail Stop 148
  NASA Langley Research Center
  Hampton, VA 23681-2199

NASA/TM-20205007197 AIAA–2020–3676

An Electrical Modeling and Thermal Analysis Toolbox for Electrified Aircraft Propulsion Simulation

Mark E. Bell
HX5, LLC, Brook Park, Ohio

Jonathan S. Litt
Glenn Research Center, Cleveland, Ohio

Prepared for the
AIAA Propulsion and Energy 2020 Forum
sponsored by the American Institute of Aeronautics and Astronautics
Virtual Event, August 24–28, 2020

National Aeronautics and
Space Administration

Glenn Research Center
Cleveland, Ohio 44135

November 2020

Acknowledgments

The authors thank the Transformational Tools and Technologies Project under NASA Aeronautics' Transformative Aeronautics Concepts Program for funding this work.

This work was sponsored by the
Transformative Aeronautics Concepts Program.

Level of Review: This material has been technically reviewed by technical management.

Available from

NASA STI Program
Mail Stop 148
NASA Langley Research Center
Hampton, VA 23681-2199

National Technical Information Service
5285 Port Royal Road
Springfield, VA 22161
703-605-6000

This report is available in electronic form at http://www.sti.nasa.gov/ and http://ntrs.nasa.gov/

An Electrical Modeling and Thermal Analysis Toolbox for Electrified Aircraft Propulsion Simulation

Mark E. Bell
HX5, LLC
Brook Park, Ohio 44142

Jonathan S. Litt
National Aeronautics and Space Administration
Glenn Research Center
Cleveland, Ohio 44135

Abstract

A simulation toolbox has been developed to model the electrical portions of Electrified Aircraft Propulsion (EAP) systems, including self-heating of electrical systems. Dynamic models of EAP systems often include turbomachinery, an electrical power system, and a thermal management system. These portions of the propulsion system can operate on time scales covering six orders of magnitude, which poses a challenging modeling task. Assumptions and approximations are made in an effort to capture the dynamics relevant to engine, electrical system, and thermal system interactions, while still allowing for fast simulations. These assumptions and approximations enable the electrical component models to run at the time scale of the turbomachinery, neglecting the very high frequency electrical dynamics, while demonstrating representative behavior of the end-to-end system. Thus the models execute in an acceptable time frame for what would otherwise be an extremely stiff simulation. The resulting simulations of EAP systems are appropriate for system-level control design and analysis. The objective of this paper is to present an overview of the Electrical Modeling and Thermal Analysis Toolbox (EMTAT). It will describe some of the approximations made to accommodate rapid execution, and some of the design tools that allow matching the model to component specifications. This paper will also provide some examples of EAP system modeling using EMTAT.

Nomenclature

f(x)	generic function
J	Jacobian
k	iteration
l	iteration number
n	iteration step counter
t	time
x	generic variable
X_il	generic inner loop variable
X_ol	generic outer loop variable

1.0 Introduction

Electrified Aircraft Propulsion (EAP) is rapidly becoming a topic of great interest to the aviation community. New electrified concept vehicles are being proposed for traditional missions (Refs. 1 to 4). New types of vehicles for Urban Air Mobility (UAM) missions such as air taxi service are under development (Ref. 5). The proposed power and propulsion systems for these various aircraft require a dynamic simulation capability for the end-to-end system that can be used for various purposes including: analysis of system operability and performance, evaluation of concepts of operation, investigation of failure modes and fault analysis, and for use in supervisory control design (Ref. 6). To address this need, NASA is developing a modeling toolbox built on MATLAB®/Simulink® from The MathWorks, Inc. This toolbox, known as the Electrical Modeling and Thermal Analysis Toolbox (EMTAT) provides the capability to simulate the electrical components of these EAP systems at a timescale appropriate to capture the interaction with the turbomachinery. EMTAT is compatible with the NASA-developed Toolbox for the Modeling and Analysis of Thermodynamic Systems (T-MATS) software package, (Ref. 7) which is used for simulating the turbomachinery. Together these codes enable models to be built of any of the various EAP architectures shown in Figure 1 (Ref. 8).

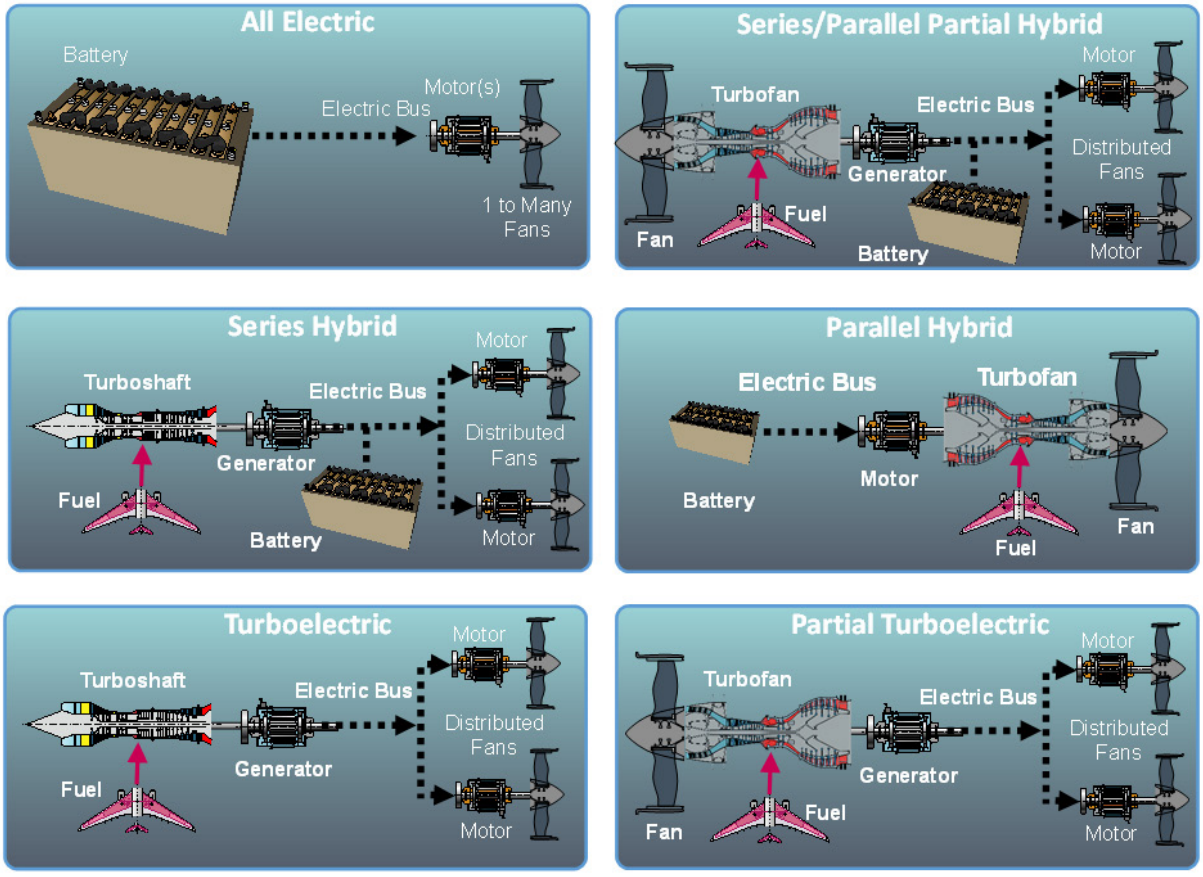

Figure 1.—Different electrified aircraft propulsion architectures.

The different architectures above all include electric motors, and either an electric generator, battery (i.e., energy storage device), or both.

- In the All Electric architecture, an energy storage device powers an electric motor which drives a fan to provide thrust. This architecture does not use turbomachinery.
- The Series/Parallel Partial Hybrid architecture uses a turbofan for both thrust and power generation. The generator extracts mechanical power from the turbofan and converts it to electrical power, which is used to drive the electric motors. The generator can also draw power from the electrical bus to act as a motor on the shaft of the turbofan, adding mechanical power instead. The energy storage device can store power from, or supply power to, the electrical bus.
- The Series Hybrid architecture uses a turboshaft engine to directly power electric motors through the generator. The attached energy storage device can store power from, or supply power to, the electrical bus.
- The Parallel Hybrid architecture uses an energy storage device to power a motor, which is used to directly add or remove torque to/from a turbofan engine that is only used for propulsion.
- The Turboelectric architecture is similar to the Series Hybrid architecture, but does not include any energy storage device.
- The Partial Turboelectric architecture is similar to the Series/Parallel Partial Hybrid architecture, but does not use an energy storage device to store or supply power.

In section 2.0, EMTAT and the different components contained therein are described. In section 3.0, examples of simulations built from EMTAT components are presented. Section 4.0 provides a summary of the paper.

2.0 EMTAT Description

The Electrical Modeling and Thermal Analysis Toolbox (EMTAT) is a set of Simulink libraries designed to simulate a variety of electrical components. Physics-based and power flow approaches are available. EMTAT is designed to interface with T-MATS as a complementary library of component models. Due to the relatively slow time step, on the order of 1 to 20 ms, of most T-MATS turbomachinery simulations, electronic devices interfaced with those simulations can be assumed to be operating at steady state from the perspective of the turbomachinery. Steady state simulations of electrical devices allow for the electrical performance calculations to be simplified, with high speed transient losses captured as a general efficiency loss. The EMTAT component models operate in steady state, and are not intended to replace high speed, high fidelity electronic simulation tools such as the Simulation Program with Integrated Circuit Emphasis (SPICE). However, since EMTAT often simulates at least an order of magnitude faster than real time, it is more useful for doing system level dynamic simulations, system level analysis, and designing and testing system-level controls. Steady state operation of electrical components, which smooth out the high speed electrical transients, demonstrates system dynamics in the operation of the integrated power and propulsion system. Physics-based and power flow models also allow for heat power loss calculations, and physics-based models allow for realistic thermal rises to be calculated, along with associated performance impacts.

In setting up simulations, EMTAT, similar to T-MATS, (Ref. 7) makes use of a generic and modifiable multiloop architecture, which contains an "outer" loop iterated over time, *t*, and an "inner" loop set up to solve for internal variable imbalances over discrete iterations, *k*. A diagram of this architecture, with a single "inner" loop (blue) and an "outer" loop (green), can be seen in Figure 2. The inner loop plant contains all components that have power imbalances, such as batteries, motors, and voltage converters. Plant imbalance measurements, or dependents, *f(x(k))*, are routed from the inner loop plant to the iterative solver. The iterative solver then adjusts the plant dependents by making changes to the inner loop plant dependent effectors, or independents, *X_il(k+1)*. In an electrical simulation, dependents often take the form of power balance errors, while each independent may specify input current demand or voltage. The iterative solver works in tandem with a "while loop" to pause the simulation at each outer loop time step, allowing the iterations to reach plant convergence (i.e., drive the dependents to zero) before the next time step. Components within the "outer" loop act to integrate the system within the time domain and may or may not be time dependent. These include outer loop effectors that feed signals from outside the "inner" loop, such as environmental conditions (e.g., ambient temperature) and system commands (e.g., bus voltage targets and speed). Controllers and other time-dependent portions of the simulation are located within the outer loop plant, which processes feedback signals from the inner loop plant, *y(t)*, to generate inner loop plant inputs, *X_ol(t+dt)*.

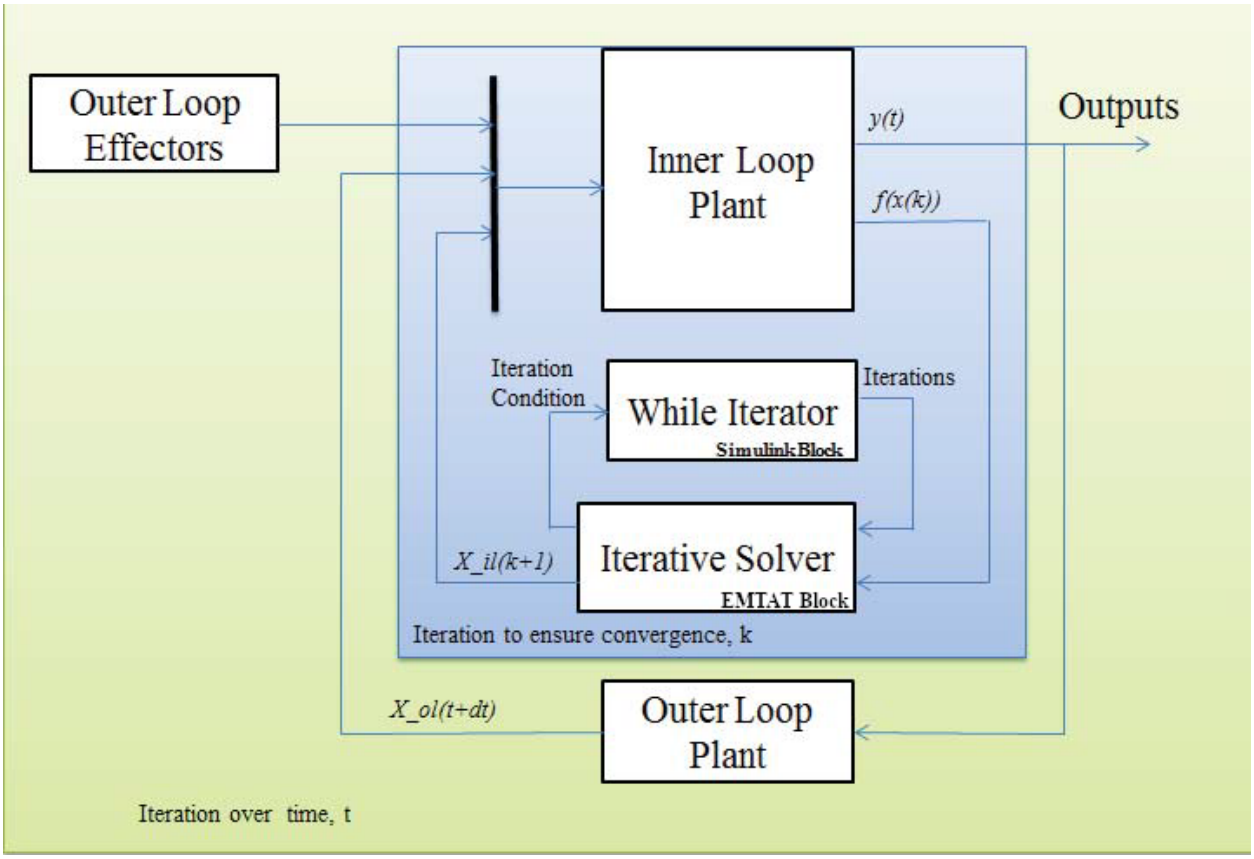

Figure 2.—EMTAT sample model architecture.

The EMTAT solvers, similar to T-MATS, (Ref. 7) are based around an iterative solver which operates with information defined by a Jacobian calculator. The iterative solver makes use of the Newton-Raphson (NR) method to step a plant toward a solution, a process described mathematically in Equation (1), where *k* is the step iteration number.

$$x(k+1) = x(k) - \frac{f(x(k))}{J} \tag{1}$$

The Jacobian (*J*) is a linear map between the inputs, *x*, and outputs, *f(x)*, of a plant and is defined by perturbing each element of *x* from its initial conditions, *x*(0), to find the effect on *f(x)*. A mathematical description of the Jacobian is given in Equation (2). For nonlinear systems, the Jacobian is only valid in a neighborhood local to the linearization point.

$$J = \begin{bmatrix} \frac{\partial f_1}{\partial x_1} & \cdots & \frac{\partial f_1}{\partial x_n} \\ \vdots & \ddots & \vdots \\ \frac{\partial f_m}{\partial x_1} & \cdots & \frac{\partial f_m}{\partial x_n} \end{bmatrix} \tag{2}$$

Equations (1) and (2) represent the two main steps of operation in an EMTAT solver. Initially, the Jacobian calculator component creates a linear representation of the plant at the current operating point. This requires perturbing slightly, in turn, each input from its initial condition, recording the results, and numerically determining the partial derivative of each output with respect to each input. The Jacobian is built from these calculations, inverted, and provided to the NR solver. In the second step, the NR solver steps toward a solution using the Jacobian developed in the first step. Because this solver method makes the assumption that the plant is locally linear, there is a chance the solver will not converge to a solution. To reduce the chances of nonconvergence, it is important to have solver initial conditions and perturbation sizes set to values appropriate for the system.

In order to increase computational speed, the Jacobian calculator is not run every time step. A Jacobian is calculated at the beginning of the simulation and is not recalculated unless the NR solver has difficulty converging. The NR solver is configurable, giving users the capability of specifying the bounds of convergence, as well as the maximum number of iterations to try in a single time step.

EMTAT utilizes Simulink's visual block-diagram modeling environment. Thus, EMTAT contains electrical component models that can be dragged and dropped into the workspace, and graphically connected to other component models to form a model of a complete electrical system. The systems created with EMTAT are modular, allowing for components to be added or removed easily. EMTAT consists of two types of component models: power flow (or load flow) and physics-based. Power flow models are based around lines linking different buses that are connected to generators or loads (Ref. 9). Power flow modeling provides a number of advantages: components may be represented by equivalent circuits that match required fidelity, and simulation execution time is fairly fast. However, these models are typically based around an efficiency map, instead of specific component parameters, and so power flow systems model efficiency losses in an empirical manner rather than relating those losses to component parameters. This aspect of EMTAT was covered in Reference 10, so the focus here will be on the physics-based component models.

Physics-based component models provide more realism through specific physical component parameters and equation based performance, and are in a sense higher fidelity than the power flow component models. These models provide realistic electrical outputs, and also calculate efficiency losses (rather than relying on a user provided map). Physics-based component models also operate in steady state from the point of view of the turbomachinery, because electrical transients are so much faster than the turbomachinery dynamics (on the scale of nanoseconds or microseconds as opposed to milliseconds). Thus, the electrical system dynamics can be ignored since any transients will have fully settled out before the mechanical system has moved appreciably. At each integration time step of the turbomachinery, the electrical system is treated as already having reached steady state. With this assumption, the integration time step can be much larger than would be the case if the electrical dynamics needed to be specifically calculated. This enables the simulation to run much faster. The electrical dynamics are still accounted for as efficiency losses, which allow the heat generated by system operation to be modeled. This steady-state modeling approach is important for the system-level applications for which EMTAT has been designed because it enables faster-than-real-time execution in most cases. Thus it lends itself to simulating missions, hardware-in-the-loop testing, and dynamic analysis of system operation. Table 1 contains a list of the component models contained in EMTAT.

The physics-based component models have a temperature input that may be used in conjunction with the Temperature Block to capture the impact of system heating on component performance. Each physics-based EMTAT component can be scaled to match user data or manufacturer specifications. Design tools are embedded in EMTAT to simplify this process for the user, predominantly the iDesign tool. iDesign provides an automated approach for calculating electrical component internal parameters that allow individual electrical components to match system level performance parameters specified by the end user. This functionality allows for the simulation of specific motors, batteries, etc., to match system performance specifications such as those typically available in product datasheets. To support design optimization studies, the physics-based models also provide a weight estimate output that is extrapolated from commercially available systems over a range of power levels.[1] All EMTAT component models are capable of bidirectional current flow, and are described in more detail below. See Appendix for specific inputs and outputs for component models included in the examples.

TABLE 1.—LIST OF COMPONENT MODELS CONTAINED IN EMTAT

Component	Power Flow Library	Physics-Based Library
Battery	Y	Y
DC Boost Converter	Y	Y
DC Buck Converter	Y	Y
Inverter/Rectifier	Y	Y
Electric Motor/Generator (PMSM)	Y	Y
Resistor	Y	Y
Transmission Line	Y	N
Super Capacitor	Y	Y
AC Transformer	Y	N
Temperature Block	N	Y

[1]Commercially available power systems were not specific to aerospace applications, and the weight data extrapolated may be higher than state of the art. Refinements to the weight estimations are planned for a later release.

1. **Battery**: This component model represents a Lithium Ion battery, and acts as a power sink or source (depending on the current demand). The output voltage is a function of the current drawn from the battery and the charge consumed (the time integral of the current drawn from the battery). Use of this model requires an external integrator block placed outside any iterative subsystem that takes in the instantaneous battery current draw, which is then fed back into the model. The battery current is solved for, such that it matches the current demand and the battery power balances.

   The iDesign tool can be used to create notional batteries given system level performance parameters, or use recorded battery discharge curves to recreate an existing design.

2. **Boost Converter**: This component model represents a generic DC-DC boost converter, controlled to produce a constant output voltage. The input current is solved for, such that the power in equals the power out (including waste heat). The system efficiency is simply the output actual power divided by the input power.

   The iDesign tool uses a set of commercial insulated-gate bipolar transistor (IGBT) datasheets in an interpolated lookup table. It selects the smallest one usable for the converter based on maximum IGBT current, which in turn is based on total power and expected ripple currents; if a current is outside the range of available data, then the system assumes a parallel combination of IGBT modules, and adjusts the parameters accordingly. To use a specific IGBT module, users can manually calculate IGBT power losses. The block parameters are generally 2-element vectors, with entries at 25 and 125 °C.[2] This allows the approximation of IGBT losses as a function of temperature.

3. **Buck Converter**: This component model represents a generic DC-DC buck converter, controlled to produce a constant output voltage. The input current is solved for, such that the power in equals the power out (including waste heat). The system efficiency is calculated from the output electrical power divided by the input power.

   The iDesign tool applies an identical approach as the Boost Converter iDesign tool described above.

4. **Inverter/Rectifier**: This component model represents a DC-to-AC inverter (for motor control) with 6 IGBTs (2 per phase) using Pulse Width Modulation (PWM) to create an output 3-phase signal (Ref. 11). When the current demand on this block is negative, it is operating as a rectifier. This block passes the torque command, speed command, and bus voltage to the motor/generator component model, and calculates parasitic power losses incurred.[3]

   The iDesign tool applies an identical approach as the Boost Converter iDesign tool described above.

[2]25 °C is a typical baseline temperature for electrical data sheets, and lower temperature extrapolation is planned for a later release.

[3]This component model may be subsumed into the motor/generator component model in a later release to simplify system modeling.

5. **Electric Motor/Generator**: This component model represents a generic AC synchronous motor whose performance is calculated in a steady state direct-quadrature (dq0) space. With a negative torque set-point, the block can be treated as a generator. The motor assumes a 3-phase inverter input, but does all of the dq0 conversions and calculations internally. This component model does not require a numeric solver to run. The motor component model comes in SI and US units.

   The iDesign tool can be used to create notional designs, based on data from commercially available devices.

6. **Resistor**: The current based resistor calculates the voltage drop across it based on current demand and resistance. No solver is needed, nor is there an iDesign feature.

7. **Transmission Line**: This component model adjusts the output voltage based on a given impedance and current demand. Currently, this component model is only available as a power flow model.

8. **Capacitor**: This component model represents a variety of capacitor types, and acts as a power sink or source depending on the current demand. The output voltage is a function of the instantaneous current drawn from the capacitor and the change in voltage. Use of this block requires an external integrator block placed outside any iterative subsystem that takes in the change in voltage, which is then fed back into the block. The capacitor current is solved for, such that it matches the current demand and the capacitor power balances.

9. **AC Transformer**: This component model performs an alternating current and voltage conversion based on a given winding ratio and impedance. Currently, this component model is only available as a power flow model.

10. **Temperature Block**: This component model takes the heat generated by any physics-based component model above and computes a thermal rise over the ambient temperature. The calculation is based on the thermal resistances and capacitances of that model, from junction to surface, and surface to ambient. These values are defined on a per-model basis, and the temperature calculation provides both a surface and junction temperature.

3.0 Examples

Due to the flexible and modular nature of EMTAT, it is impractical to show every system that could be modeled with the library. While the following examples show two basic systems, it is possible to create much more complex systems, including those with turbomachinery, which can be integrated with T-MATS.

The first example is of a physics-based battery block, comparing performance with and without temperature feedback. Temperature feedback allows users to see the performance changes associated with changing temperatures in the components. Figure 3 shows a simple battery charge/discharge simulation, using the physics-based battery block (yellow) and the heat-to-temperature block (red) for temperature feedback. The battery is a generic lithium ion battery, with a nominal voltage of 3.3 V and a capacity of 2.3 A-hours. The system discharges at 9.2 A until the battery reaches 5 percent State of Charge (SOC), then charges the battery at 9.2 A (represented by a negative current demand) until it reaches 95 percent SOC, and repeats. The heat-to-temperature block accepts inputs of heat generated by the battery, Heat_Generated, and ambient temperature, T_ambient, and produces surface and junction temperature outputs. These temperatures are then averaged and provided as a temperature feedback input supplied to the battery block, T_avg(C). If desired, a user can forego the calculation of a temperature feedback signal and simply supply a constant temperature as an input to the battery block. Figure 4 shows a battery charge/discharge simulation outputs without temperature feedback, Figure 5 shows the same simulation outputs but using temperature feedback to modify the performance. As can be seen by comparing the figures, both simulations provide realistic battery performance curves, including lithium ion characteristic voltage hysteresis. The temperature feedback causes increased internal temperatures, leading to increased heat generation and faster discharge cycles. Internal temperatures affect physical component properties as specified by manufacturer data sheets.

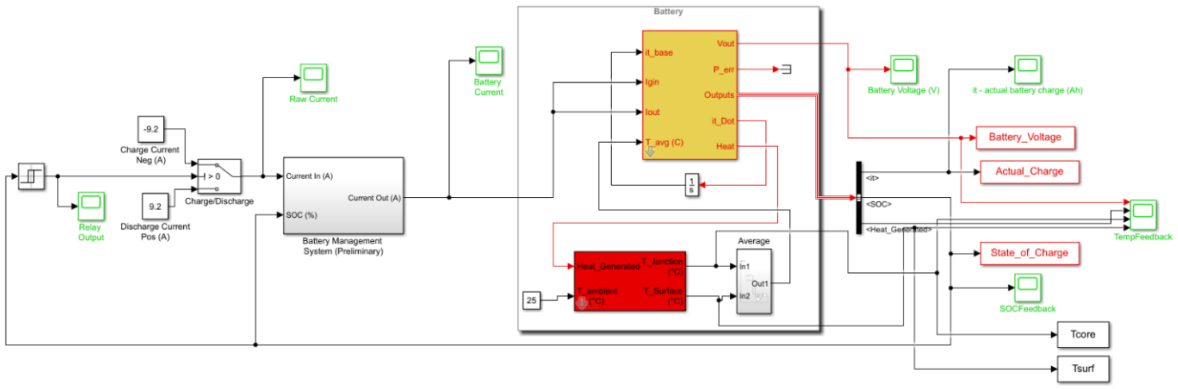

Figure 3.—EMTAT battery charge/discharge diagram.

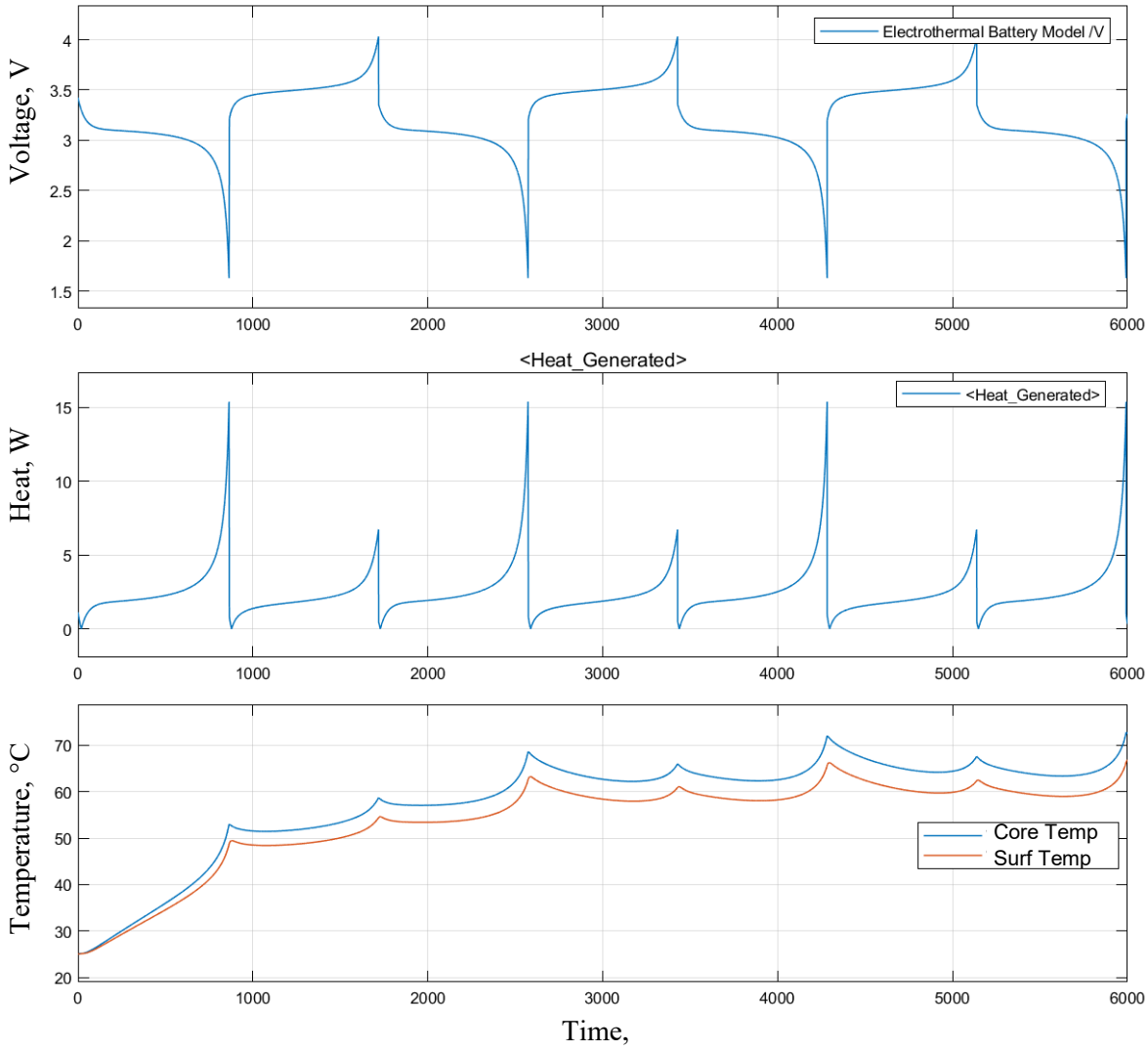

Figure 4.—Battery charge/discharge simulation without temperature feedback. The top subplot shows the battery voltage over the simulation, and the middle subplot shows the heat generated in the battery over the simulation. The bottom subplot shows the calculated core temperature (blue) and surface temperature (orange). The battery completes four full discharge cycles with three full charge cycles over the 6000 s run time, reaching a peak core temperature of just over 70 °C.

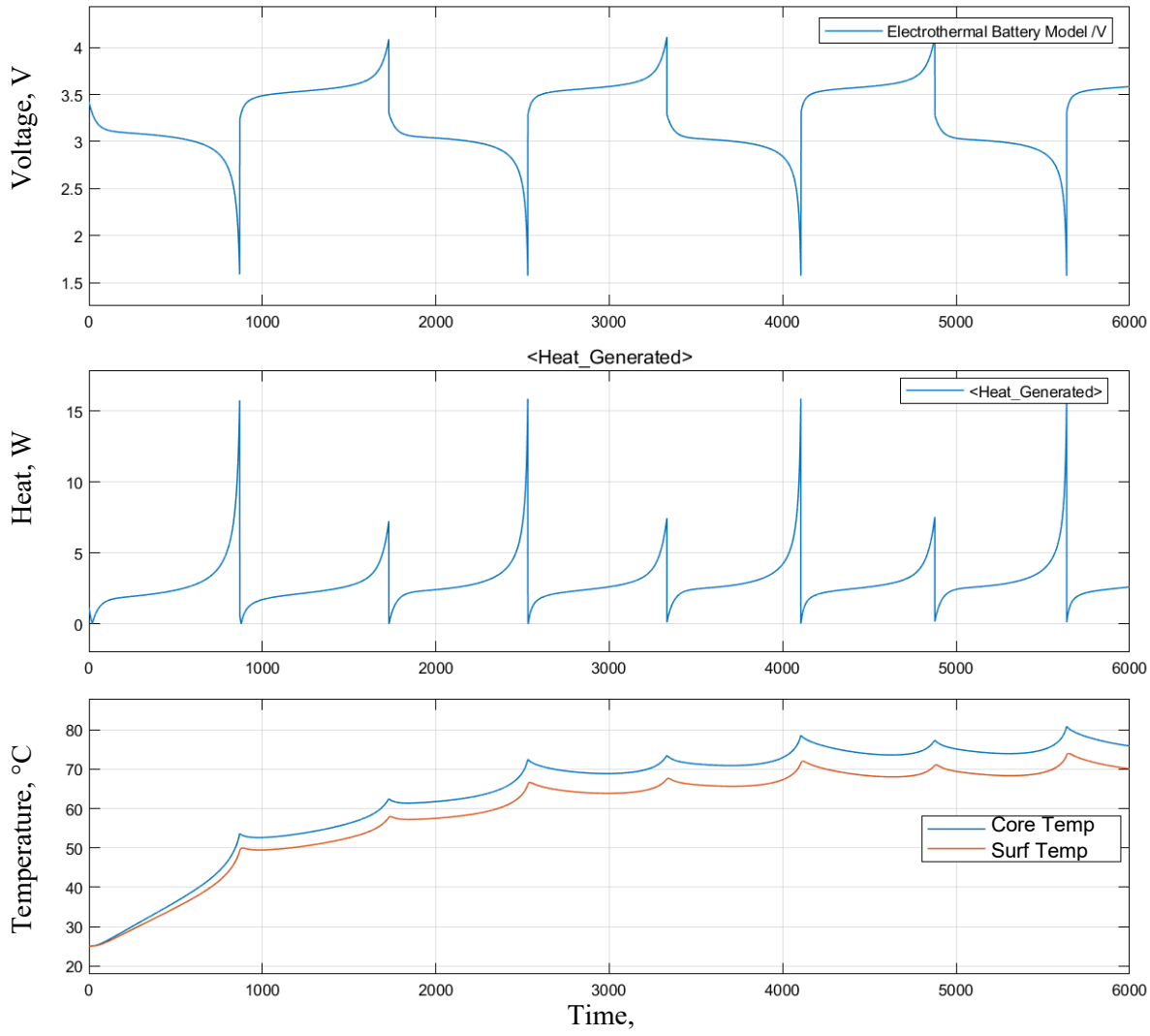

Figure 5.—Battery charge/discharge simulation with temperature feedback. The top subplot shows the battery voltage over the simulation, and the middle subplot shows the heat generated in the battery over the simulation. The bottom subplot shows the calculated core temperature (blue) and surface temperature (orange). The battery completes four full discharge cycles with three full charge cycles and an additional partial charge cycle over the 6000 s run time, reaching a peak core temperature of just over 80 °C.

The next example is an inverter/rectifier and motor/generator system, with the output of the motor/generator controlled through a torque set-point. Figure 6 shows this system setup using the T-MATS Steady State Newton Raphson Solver with Jacobian Calculations (Ref. 7). (All T-MATS component models and solvers are compatible with EMTAT.) The stator voltage of the motor is compared to the RMS value of the fixed bus voltage for the solver input. The solver outputs motor speed to the system, and the torque is prescribed as a ramp from 50 to –50 N-m through the 100 s simulation. When an electric motor shaft is turned mechanically, it begins to generate current instead of using current to turn the shaft. This mechanical power consumption is represented as a negative torque output command. As all of the EMTAT blocks support bidirectional current and power flow, when the commanded torque of the motor goes negative, the system calculates a negative current demand, which is treated in EMTAT component models as electrical power generation.

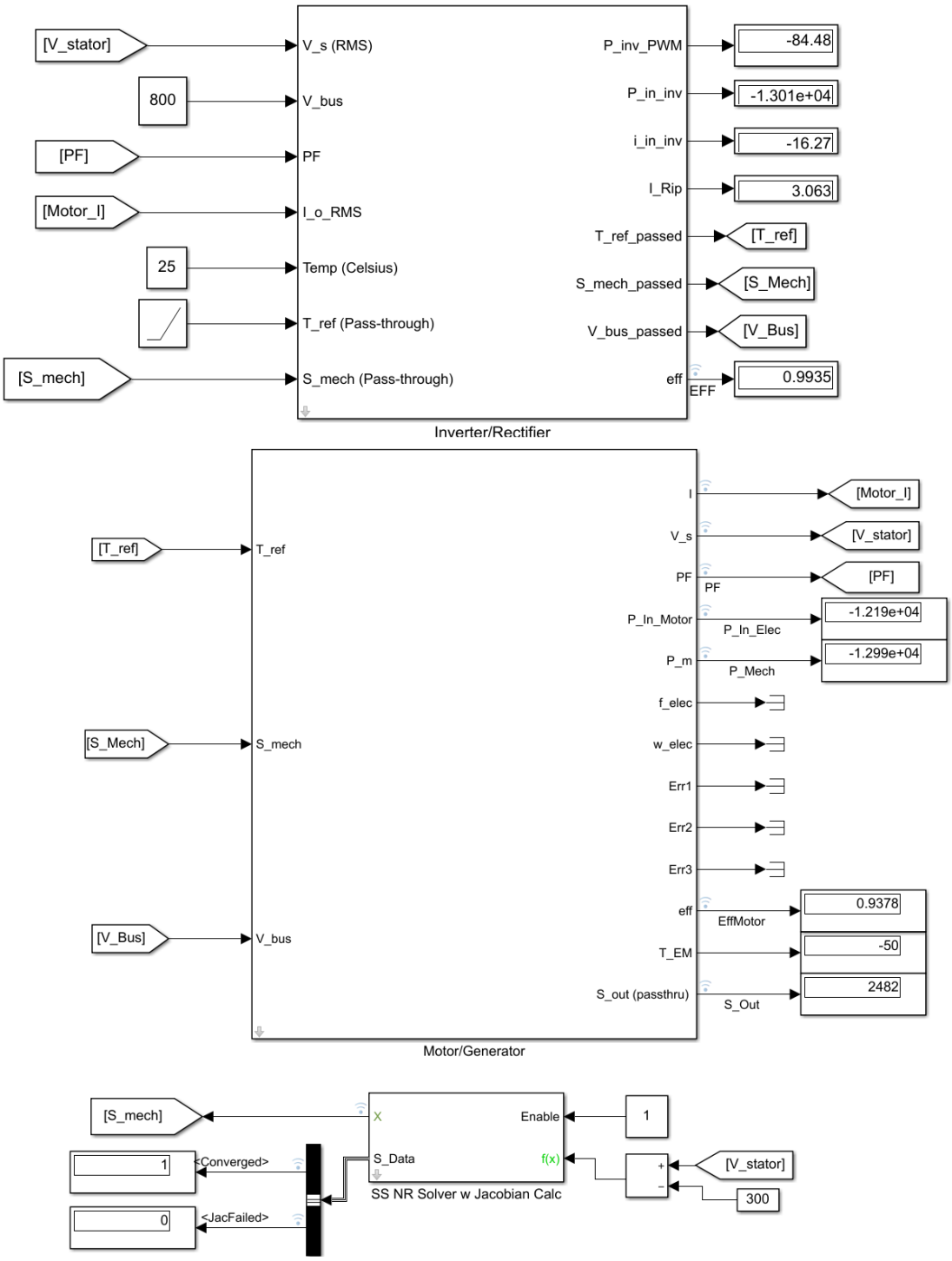

Figure 6.—Inverter/rectifier and motor/generator in the torque control mode.

The inverter/rectifier and motor/generator component model parameters were calculated using the iDesign tools, and the iDesign inputs are shown in Table 2. As can be seen in Figure 7, the motor efficiency (based on power losses) and power factor (based on dq0 voltage and current) update dynamically, with discontinuities as the mechanical power and input currents cross zero. Since these are calculated values for output reference only, and are not used in any internal calculations, their discontinuities do not affect the overall simulation. Likewise, as can be seen in Figure 8, the input motor electrical power and output motor mechanical power both move from positive to negative, as does the input motor current. As is typical in real electric motor-generator systems with nonzero efficiency losses, the motor requires more electrical power input than it provides in mechanical output, and vice versa when generating. This example controls the system using the solver and basic constants, but can be adapted to much more complex systems and include the integration of controls.

TABLE 2.—INVERTER/RECTIFIER AND MOTOR/GENERATOR IDESIGN TOOL INPUT VALUES

Inverter/Rectifier Input	Inverter/Rectifier Value	Motor/Generator Input	Motor/Generator Value
Maximum Power (W)	22000	Number of poles	4
Maximum Phase Voltage (V)	400	Stator Resistance (Ohm)	.032
F_sw (0 to default to max, Hz)	0	Stator Inductance (H)	.00086+0.00029
Stator inductance of motor (H)	.00086+0.00029	Nominal Speed (RPM)	3000
		Maximum/Nominal reference torque (Nm)	70
		Maximum output power (W)	22000
		Current Limit (A)	36.5
		Input Power Limit (W)	30000
		Back EMF Constant (V/kRPM)	121
		Nominal Voltage (V)	368
		Maximum allowable torque (Nm)	80
		Iron Loss Calculation	Compute iron losses automatically
		Nominal Current (A)	36.5
		Nominal Power Factor	0.99

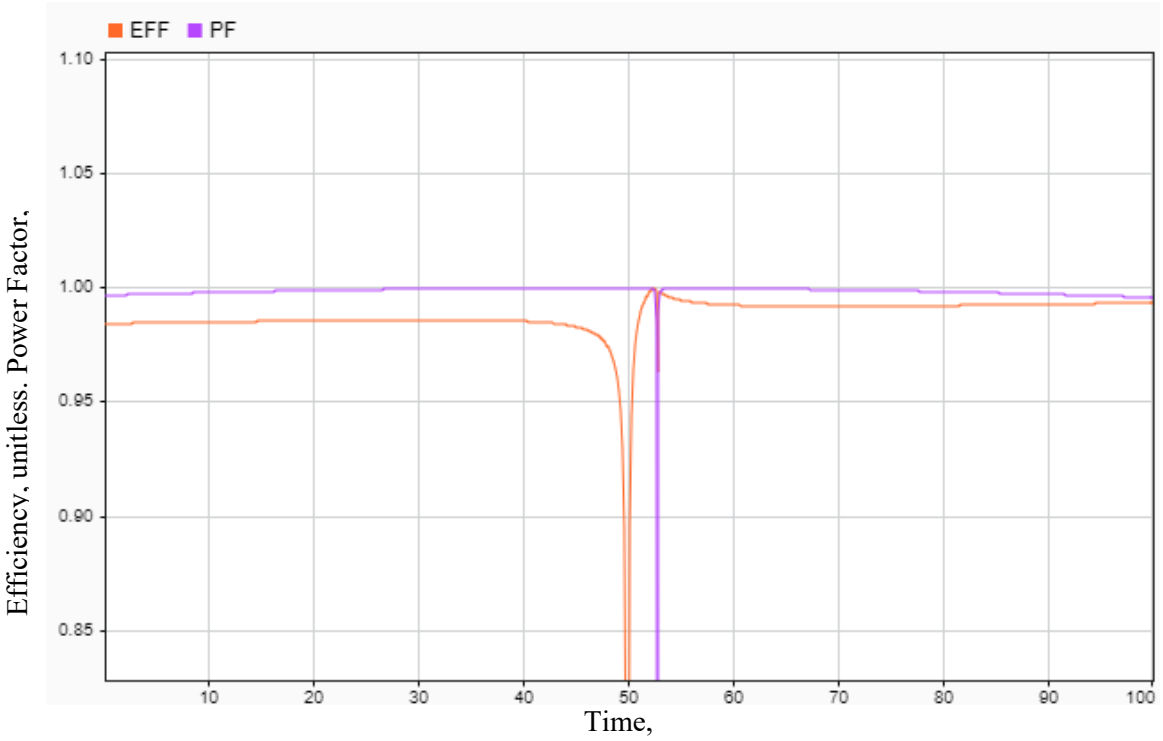

Figure 7.—Efficiency (EFF, orange) and Power Factor (PF, purple) vs. time. Discontinuities as the system moves from power usage to power generation are represented, but these do not impact the system itself as they are calculated values.

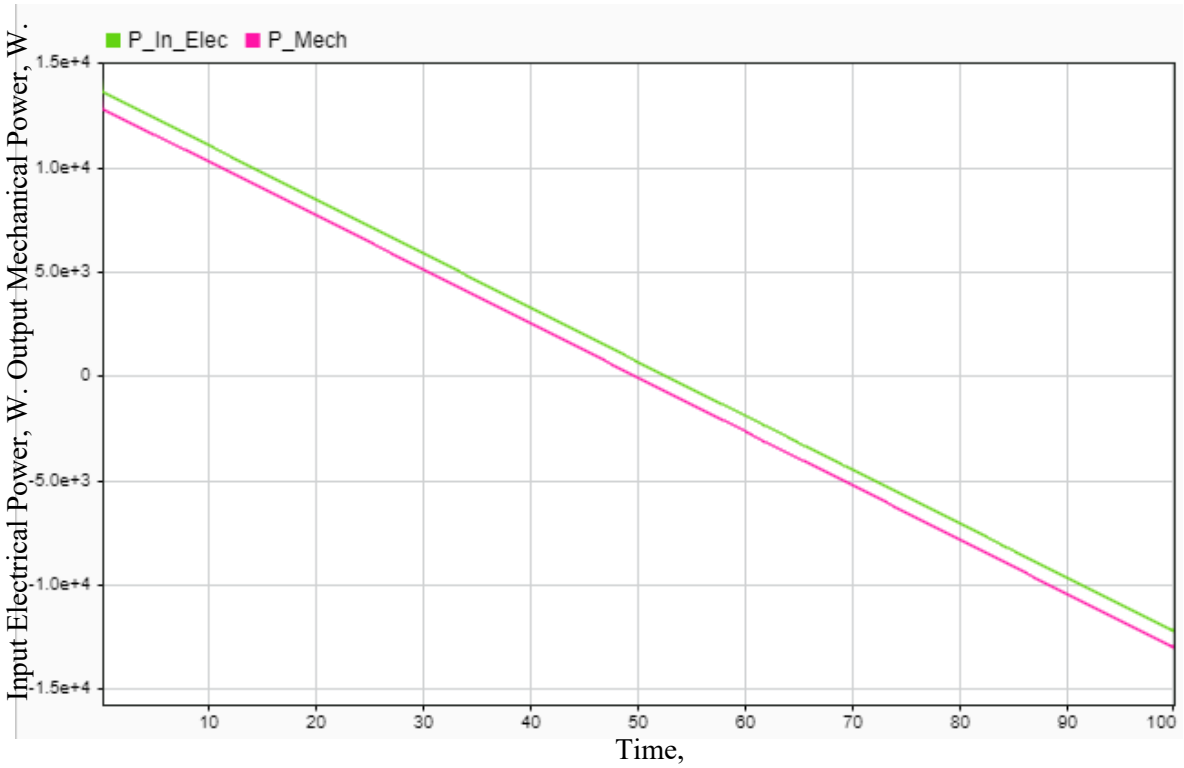

Figure 8.—Input Electrical Power (P_In_Elec, green) and output mechanical power (P_Mech, pink) vs. time. Note that there are no discontinuities in the input power or output power as the system moves from power usage to power generation.

4.0 Summary

The Electrical Modeling and Thermal Analysis Toolbox (EMTAT) is an open source MATLAB/Simulink toolbox that provides simple to use modeling and simulation tools to facilitate control design, analysis, evaluation, and virtual testing of electrified aircraft propulsion concepts. This paper provides an introduction to the EMTAT software package. The provided examples illustrate a battery with thermal feedback, and a torque controlled inverter-motor pair moving from power usage to power generation. Realistic parameter changes due to thermal states and dynamic transients are demonstrated. The examples do not fully demonstrate all of the capabilities offered by EMTAT. Thus, it is important to note that this toolbox can be adapted to a wide variety of electrical system modeling problems that go well beyond what has been demonstrated in this paper.

Appendix—Inputs and Outputs of Select Physics Based Blocks

The EMTAT component models have a variety of inputs and outputs that may not be immediately obvious to the user. This appendix describes all of the inputs and outputs of the EMTAT physics based blocks that were used in the examples provided in this paper. For a full and updated list of parameters for all blocks, readers are referred to the EMTAT software repository, which will be located in the NASA GitHub at https://github.com/nasa/EMTAT. This is planned to be publicly released by the end of September 2020.

BATTERY PARAMETERS	**PARAMETER DESCRIPTION**
E0_M	Battery constant voltage (V)
Q_M	Battery capacity (Ah)
R_M	Battery internal resistance (ohm)
K_M	Polarization constant (Ah^-1)
A_M	Exponential zone amplitude (V)
B_M	Exponential zone time constant inverse (Ah^-1)
SOC_Init_M	Initial percentage state of charge (%)
battery_type_M	Li-Ion, Ni-MH, or Lead Acid based. Currently only Li-Ion supported.
INPUT SIGNAL NAME	**INPUT SIGNAL DESCRIPTION**
it_base	Charge being consumed
IgIn	Input current guess
Iout	Required output current
OUTPUT SIGNAL NAME	**OUTPUT SIGNAL DESCRIPTION**
Vout	Output voltage
P_err	Output power error
Outputs	Output current, power, state of charge, charge being consumed, derivative of charge consumption, and heat generation
it_Dot	Derivative of charge consumption
Heat	Generated heat in watts

TEMPERATURE BLOCK PARAMETERS	**PARAMETER DESCRIPTION**
Tj_0_M	Initial Junction Temperature
Ts_0_M	Initial Surface Temperature
Cj_M	Lumped Heat Capacity at Junction (J/K)
Rj_M	Conduction Resistance b/w junction and surface (K/W)
Cs_M	lumped heat capacity at surface (J/K)
Ru_M	Convection resistance b/w surface and cooling flow (K/W)
INPUT SIGNAL NAME	**INPUT SIGNAL DESCRIPTION**
Heat_Generated	Heat generated by the device/component
T_ambient	Ambient temperature

OUTPUT SIGNAL NAME	OUTPUT SIGNAL DESCRIPTION
T_Junction	Junction temperature calculated based on inputs and physical parameters given above
T_surface	Surface temperature calculated based on inputs and physical parameters given above

INVERTER/RECTIFIER PARAMETERS	PARAMETER DESCRIPTION
T_M (temperature breakpoints)	These are 2-vector coefficients relating to a linear relationship between power losses and current, which is also adjusted by a linear temperature relation. See the source from element14.com for details on how these are obtained.
u_D_M	
u_ce0_M	
R_c_M	
R_D_M	
E0_M	Same as the above, but for switching energy. This *can* vary with temperature, but does not in the included IGBT models
E1_M	
f_sw_M	Frequency at which the IGBTs can switch in Hz
L_s_M	Stator inductance of the attached motor (H), used in ripple current computation
INPUT SIGNAL NAME	**INPUT SIGNAL DESCRIPTION**
V_s (RMS)	RMS Stator voltage from attached motor
V_batt	Battery voltage (DC power voltage) (V) (Pass-through)
PF	Power factor of attached motor
I_o_RMS	RMS Current (from motor) (A)
Temp (Celsius)	IGBT temperature (Celsius)
T_ref	Torque (pass-through), use units appropriate for motor
S_mech	Speed (RPM, pass-through)
OUTPUT SIGNAL NAME	**OUTPUT SIGNAL DESCRIPTION**
P_inv_PWM	Inverter losses due to IGBTs
P_in_inv	Calculated input power to inverter
I_in_inv	Calculated inverter input current
I_rip	Ripple current
T_ref passed, S_mech_passed, V_batt_passed	Input quantities passed straight through to motor
eff	Efficiency of inverter
iDesign	**iDesign input description**
P_max_I	Maximum inverter power
V_phase_I	Maximum phase voltage
f_sw_I	Switching Frequency (set to 0 to default to max IGBT f_sw)
L_s_I	Stator inductance of the attached motor (H), used in ripple current computation

MOTOR/GENERATOR PARAMETERS	PARAMETER DESCRIPTION
pp	Number of poles in motor divided by 2
flux_m	Permanent magnet flux linkage (Weber)
R_s	Resistance of stator winding (Ohms)
L_s	Inductance of stator winding (H)
P_Fe_Nom	Iron losses at nominal speed on spec. sheet (W)
S_nom	Nominal speed for specifications (RPM)
T_nom	Nominal torque (Nm)
P_out_max	Maximum output power (W)
I_max	Maximum current through motor (A)
P_in_max	Maximum input power (W)
T_max	Maximum allowable torque (Nm)
INPUT SIGNAL NAME	**INPUT SIGNAL DESCRIPTION**
T_ref	Load torque (Nm)
S_mech	Speed (RPM)
V_batt	DC power source voltage
OUTPUT SIGNAL NAME	**OUTPUT SIGNAL DESCRIPTION**
I	Phase current (RMS)
V_s	Stator voltage (V)
PF	Power factor
P_in_Motor	Input power to motor (W)
P_m	Power output by shaft (Torque*speed) (Nm)
f_elec	Electrical frequency (Hz)
w_elec	Angular electrical frequency (rad/s)
Err1	1 if I>I_max, else 0
Err2	1 if V_s > (V_batt/sqrt(2)), else 0
Err3	1 if P_in_Motor>P_in_max, else 0
eff	Efficiency of motor
T_EM	Electromagnetic torque produced by motor (Nm)
S_out	Output speed (passed through from S_mech) (RPM)
I_nom_i	Nominal current (for iron loss computation) (A)
PF_nom_i	Nominal power factor (for iron loss computation)
P_Fe_Calc_Flag	Internal variable

References

1. Bradley, M.K., and Droney, C.K., "Subsonic Ultra Green Aircraft Research: Phase II—Volume II—Hybrid Electric Exploration," NASA/CR—2015-218704, 2015.
2. Schiltgen, B.T., Freeman, J.L., and Hall, D.W., "Aeropropulsive Interaction and Thermal System Integration within the ECO-150: A Turboelectric Distributed Propulsion Airliner with Conventional Electric Machines," AIAA Aviation Technology, Integration and Operations Conference, AIAA-2016-4064, AIAA, Reston, VA, 2016.
3. Welstead, J., and Felder, J.L., "Conceptual Design of a Single-Aisle Turboelectric Commercial Transport with Fuselage Boundary Layer Ingestion," 54th AIAA Aerospace Sciences Meeting, AIAA, Reston, VA, 2016.
4. Felder, J.L., Brown, G.V., and Kim, H.D., "Turboelectric Distributed Propulsion in a Hybrid Wing Body Aircraft," 20th International Society for Airbreathing Engines, ISABE-2011-1340, Gothenburg; Sweden, 2011.
5. Silva, C., Johnson, W., Antcliff, K.R., Patterson, M.D., "VTOL Urban Air Mobility Concept Vehicles for Technology Development," AIAA-2018-3847, AIAA AVIATION Forum, June 25-29, 2018, Atlanta, Georgia.
6. Connolly, J.W., Chapman, J.W., Stalcup, E.J., Hunker, K.R., Chicatelli, A.K., Thomas, G.L., "Modeling and Control Design for a Turboelectric Single Aisle Aircraft Propulsion System," AIAA-2018-5010, AIAA Propulsion and Energy Forum, July 9-11, 2018, Cincinnati, Ohio.
7. Chapman, Jeffryes W., Lavelle, Thomas M., May, Ryan D., Litt, Jonathan S., Guo, Ten-Huei, "Propulsion System Simulation Using the Toolbox for the Modeling and Analysis of Thermodynamic Systems (T-MATS)," AIAA 2014-3929, 50th AIAA/ASME/SAE/ASEE Joint Propulsion Conference, Cleveland, OH, July 28-30, 2014.
8. Adibhatla, S., et al., "Propulsion Control Technology Development Needs to Address NASA Aeronautics Research Mission Goals for Thrusts 3a and 4" AIAA-2018-4732, AIAA Propulsion and Energy Forum 2018; July 07, 2018 - July 13, 2018; Cincinnati, OH.
9. Gross, C.A., Power System Analysis, John Wiley & Sons, New York, NY, 1998.
10. Chapman, J.W., Litt, J.S., "An Approach for Utilizing Power Flow Modeling for Simulations of Hybrid Electric Propulsion Systems," AIAA 2018-5018, AIAA/IEEE Electrified Aircraft Technology Symposium, July 12-13, 2018, Cincinnati, OH.
11. Mapelli, F.J., and Tarsitano, D., "Modeling of Full Electric and Hybrid Electric Vehicles," New Generation of Electric Vehicles, Zoran Stevic, IntechOpen, DOI: 10.5772/53570, London, England, 2012.